Front. Optoelectron. 2014, 7(4): 493–500
DOI 10.1007/s12200-014-0360-3

RESEARCH ARTICLE

Improved pilot data aided feed forward based on maximum likelihood for carrier phase jitter recovery in coherent optical orthogonal frequency division multiplexing

Jean TEMGA (✉), Deming LIU, Minming ZHANG

National Engineering Laboratory for Next Generation Internet Access System, Huazhong University of Science and Technology, Wuhan 430074, China

Abstract Pilot data aided feed forward (PAFF) carrier recovery is essential for phase noise tracking in coherent optical receivers. This paper describes a new PAFF system based on new pilot arrangement and maximum likelihood (ML) to estimate the phase jitter in coherent receiver-induced by local oscillator's lasers and sampling clock errors. Square M-ary quadrature amplitude modulation (M-QAM) (4, 16, 64, and 256) schemes were used. A detailed mathematical description of the method was presented. The system performance was evaluated through numerical simulations and compared to those with noise-free receiver (ideal receiver) and feed forward without ML. The simulation results show that PAFF performs near the expected ideal phase recovery. Results clearly suggest that ML significantly improves the tolerance of phase error variance. From bit error rate (BER) sensibility evaluation, it was clearly observed that the new estimation method performs better with a 4-QAM (or quadrature phase shift keying (QPSK)) format compared to three others square QAM schemes. Analog to digital converter (ADC) resolution effect on the system performance was analyzed in terms of *Q*-factor. Finite resolution effect on 4-QAM is negligible while it negatively affects the system performance when *M* increases.

Keywords coherent optical orthogonal frequency division multiplexing (CO-OFDM), phase noise, feed forward (FF), maximum likelihood (ML), phase error variance, bit error rate (BER), *Q*-factor

1 Introduction

Coherent optical modems have been the main focus in optical industry in recent years because of increasing demands of data rate driven by the application of new technologies and the exponential growth of electronic processing speeds [1,2]. Using multicarrier modulation technique like orthogonal frequency division multiplexing (OFDM) with coherent detection is more attractive for future optical transmission system. This combination of coherent detection and OFDM modulation improves the chromatic dispersion and polarization mode dispersion (PMD) estimation and mitigation. Secondly, the overlaps of OFDM subcarriers result in high optical spectral efficiency [3]. Moreover, when combined with square M-ary quadrature amplitude modulation (M-QAM) constellation, coherent optical orthogonal frequency division multiplexing (CO-OFDM) can meet the growing need for higher spectral efficiencies in future optical transport system [4]. However, one of the most severe impairment that affects coherent systems employing high-order modulation formats is the presence of phase noise and sampling clock errors [5,6].

Besides phase noise and sampling errors, phase jitter induced by sampling clock errors in analog digital converter (ADC) and local oscillator (LO) lasers phase noise is considered to have markedly negative impact on coherent receivers as reported in previous literature [7]. Without digital signal processing (DSP) for phase recovery, the phase jitter in the receiver can destroy the orthogonality among the OFDM subcarriers [8,9]. Hence, the phase jitter must be estimated and compensated, especially for optical OFDM receivers. So far, there are only a few reports on this issue which compensate individually sampling clock errors and lasers phase noise. One way is compensating the sampling clock errors

Received July 8, 2013; accepted December 31, 2013

E-mail: Jeantemga4@gmail.com

by re-sampling in the time domain [10] and transmitting a dedicated clock signal [11,12]. Re-sampling requires interpolation of sample points while transmitting a dedicated clock signal needs more circuits in the transmitter. Another way is the compensation of the lasers phase noise. For this issue, many algorithms have been introduced; such as common phase error (CPE) based [13] and radio frequency-pilot (RF-pilot) [14] based phase noise compensation which shows a superior tolerance to phase noise, compared to the first method, independent of the symbol length. These compensation methods mitigate either sampling errors or phase noise, which are two causes of phase jitter impairment.

In this paper, we comprehensively studied for the first time the carrier phase noise jitter (PNJ) as an impairment resulting from the combination of sampling clock errors and local oscillator phase noise at a CO-OFDM receiver. We assumed there was perfect chromatic dispersion compensation, which could be considered as a jitter source [8]. We evaluated the phase estimation based on a new system of diagonal pilot arrangement in the transmitter and a feed forward (FF) scheme which re-uses the pilot subcarriers in the receiver. Then the study was extended to maximum likelihood (ML) phase noise compensation systems employing arbitrary M-QAM constellations. A comparative analysis of feed forward maximum likelihood (FFML) with a pilot-data-aided algorithm using high square QAM modulation formats 4-QAM or quadrature phase shift keying (QPSK), 16-QAM, 64-QAM and 256-QAM was studied. This analysis was conducted at an Optisystem simulation platform in the presence of the random phase errors due to sampling errors in ADC, local oscillators' lasers phase noise and additive channel noise. Except some additional DSP mathematical computation resources, the new phase jitter compensation method does not require additional hardware. This paper is divided into five sections including this introduction as Section 1. Section 2 describes the system architecture and mathematical model used for digital signal processing (DSP) in CO-OFDM. The main principles of new pilots' arrangement in OFDM frame and FFML are detailed in Section 3. Section 4 highlights simulation conducted at an Optisystem platform to quantify the performance of the new estimation system. Section 5 provides a summary on the results of this study.

2 System architecture and mathematical model in CO-OFDM

2.1 System architecture

Figure 1 shows the CO-OFDM transmission system with DSP. The transmitter DSP helps to perform the following tasks: data conversion from serial to parallel, pulse shaping for symbols mapping onto M-QAM modulation format, inverse fast Fourier transform (IFFT) to convert signal from frequency to time domain, guard interval (GI) insertion to avoid inter symbol interference (ISI) and insertion of pilots for channel estimation at the receiver. Two ADC [15] are used to convert the time-domain digital signal to analog signal. A pair of electrical low-pass filters is used to remove the alias sideband signal. A radio-to-optical (RTO) up- converter transforms electrical signal into the optical domain using an inphase/quadrature (I/Q) optical modulator made by two Mach-Zehnder modulators (MZMs) and an 90° optical phase shifter.

At the receiver, the coherent OFDM optical-to-radio (OTR) front-end integrates local oscillator, balanced photo detectors to provide two signals corresponding to I and Q components filtered by low pass filters (LPF) [15]. These baseband signals are then sampled at their Nyquist rate by ADC where sampling errors occur. The DSP compensates for any impairment at the receiver and channel impairments (chromatic dispersion, polarization mode dispersion), and fiber non linear (NL) impairments.

This paper focuses on receiver impairment such as PNJ induced by LO lasers and sampling clock errors. Fiber channel impairments (chromatic dispersion and polarization dispersion) are beyond the scope of this study. We only considered the PNJ caused by the instantaneous phases of the transmitter LO lasers unlocked from each other, as well as circuit clock errors.

2.2 Mathematical description and phase jitter model

We have reported in previous research [16] that in the presence of PNJs after the fast Fourier transform (FFT) in coherent OFDM receiver, the received signal is expressed as

$$R_m(k) = \theta_0 H_m(k) X_m(k) + I_m(k) + N_m, \qquad (1)$$

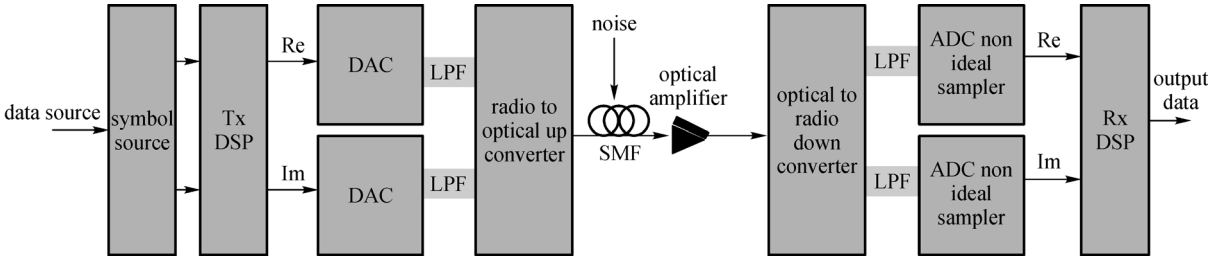

Fig. 1 Architecture of digital signal processing-based CO-OFDM

where

$$\theta_0 = \frac{1}{N} e^{j[\omega_{LD}(t+\varepsilon)+\phi_{LD}]} \sum_{n=0}^{N-1} e^{\frac{j2\pi l\varepsilon_n}{T}}, \quad (2)$$

$$I_m = \sum_{k=0,k\neq m}^{N-1} H_m(k) X_m(k) \sum_{n=0}^{N-1} \theta_{k-m} e^{\frac{j2\pi}{N}(k-m)n}, \quad (3)$$

where θ_0 is the optical OFDM transmitter/receiver phase noise, including optical and radio frequency (RF) local oscillator noise, and $X_m(k)$ is the transmitted baseband OFDM signal, $H_m(k)$ is overall end-to-end OFDM link impulse response function, N_m is presumably white Gaussian noise which is the optical noise added from the optical amplifier throughout the optical fiber link. The fiber nonlinearity is not considered in this paper.

Considering the assumptions of free inter-symbol interference (ISI) and no fiber nonlinearities, Eq. (1) can be written as follows

$$R_m(k) = \theta_0 H_m(k) X_m(k) + N_m. \quad (4)$$

From Eq. (2), it is noticed that transceiver and receiver oscillators phase noise contributions are located in the phase rotation term summing their individual phases. It should be noted that this is close to the real scenario since transceiver (Tx) and receiver (Rx) oscillators lasers cannot be located together because of chromatic dispersion. From this point on, the combined Tx and Rx lasers phase noise could be defined as

$$\theta_0(nT_s) = \theta_{Tx}(nT_s) + \theta_{Rx}(nT_s) + \theta_N(nT_s), \quad (5)$$

where $\theta_N(nT_s)$ is due to filtered noise.

It is assumed that frequencies of signal and LO lasers are synchronized so that the time variation in $\theta_N(nT_s)$ is due to phase noise only, which can be modeled as a Wiener process [17].

$$\theta_0(kT_s) \equiv \theta_k = \sum_{n=-\infty}^{k} f_n. \quad (6)$$

Let's assume at time $t = 0$, phase $\theta_0 = 0$. For a Wiener process, at any time $t = \Delta t$, the phase deviates from 0, and the phase difference measured over Δt is a Gaussian random variable.

In Eq. (6), the increments f_n are independent and identically distributed Gaussian random variables with zero mean and variance:

$$\sigma_\theta^2 = 2\pi(\Delta f \cdot T_s), \quad (7)$$

where Δf is the sum of the linewidth of transmitter laser and receiver local oscillator laser.

3 Principles of pilot data aided feed forward and feed forward maximum likelihood

3.1 Pilot data aided feed forward

In Fig.2, we denote by

N_s	OFDM symbols numbers in one OFDM frame;
N_{sb}	Number of subcarriers in one OFDM symbol;
i	OFDM index of subcarriers in the frame ($i = 1,2,...,N_{sb}$);
k	OFDM index of symbols in the frame ($k = 1,2,...,N_s$);
$X_{k,i}$	Position of subcarriers inside the frame;
$p_{k,i}$	Position of pilots inside the frame.

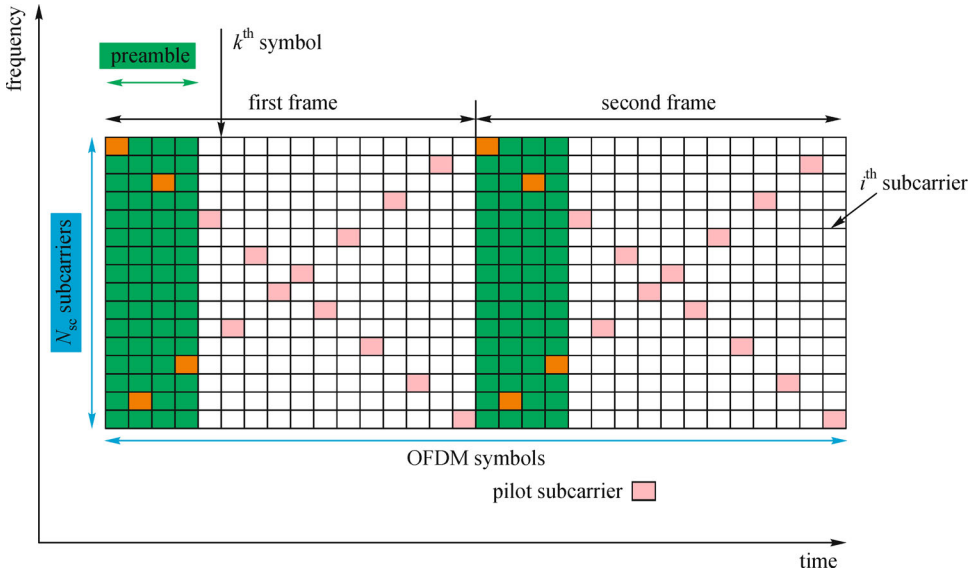

Fig. 2 Pilots arrangement for carrier phase jitter recovery (CPJR)

Pilots' positions are defined as follows:

For $k \in [1;N_s]$ and $i \in [1;N_{sb}]$, the pilots' positions are given by the following mathematical expression:

$$p_{k,i} = p_{mN_s+k,i} = \begin{cases} X_{k,i}, & i = k = 2m+1, \\ X_{k,N_{sb}-k+1}, & k = 2m,\ i = N_{sb}-k+1, \end{cases}$$

where m is an integer.

The main idea behind the novel pilot arrangement method is the insertion of pilots at transmitter in time-frequency optical OFDM frame space in the two congruent diagonals, such as shown in Fig. 2. Pilots are dispersed only in the two diagonals.

Such subcarriers allocation assigns the pilot subcarriers to all OFDM symbols across the entire signal spectrum, thus leading to highly accurate, interpolation-free phase estimation. The fact that one symbol contains a single pilot subcarrier, results in the same number of pilots in each frame as the number of data subcarriers within each symbol. This result is buffer-free flow. As the set of pilot is usually short, from a few data to a few symbols, a FF approach is suggested to speed up the required estimation process. The above mentioned features are totally different from those associated with block pilot insertion and comb pilot used in wireless communications.

Figure 3 illustrates the physical framing structure, where pilots are inserted for our carrier phase jitter estimation. One can see how pilots represent one symbol in a whole frame structure.

During the transmission, the pilot is impaired by the

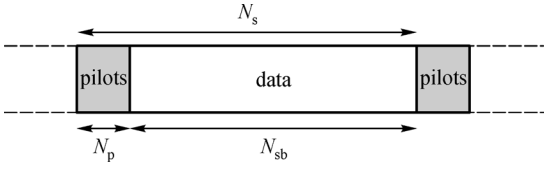

Fig. 3 Physical framing structure of CO-OFDM signal with regularly inserted pilot symbol

oscillators phase noise from both transmitter and receiver. The phase shift that occurs because of this impairment in a noise-free environment could be the same as the oscillators' phase noise collected from data symbols. At the receiver, pilots are filtered out by low-pass filter and their phase is determined.

According to Eq. (5), we deducted the instantaneous pilot phase inserted in a symbol at the transceiver for estimation. It is written as

$$\theta^{(p)} = \theta^p_{Tx}(t) + \theta^p_{Rx}(t) + \theta^p_N(t). \tag{8}$$

Equation (5) is written with a discrete time index but a continuous time invariable t is employed throughout Eq. (8) simply because the discrete time processing at Nyquist rate is equivalent to continuous-time processing [18].

From Eq. (8), the receiver can easily estimate the pilot phase as $\hat{\theta}^{(p)}$, where the estimation error will depends on $\theta^p_N(t)$. Then the receiver will de-rotate the received signal term in Eq. (4).

3.2 Principle with maximum likelihood

As we mentioned above, the phase noise is due to the linewidth difference between the transmitter and receiver lasers. The data pilot aided technique presented in this paper makes use of phase estimate carried out over the pilot set. As the symbol transmitted over the pilots is known, it is clear that the best estimator that can be used there is the ML estimator. For CO-OFDM, we assumed that N_p subcarriers are used as pilot subcarriers to estimate the phase noise. The ML of phase noise jitter is calculated as shown in Fig. 4. It calculates an estimate $\hat{\theta}^{(p)}_{ML}$ for the residual phase noise uncompensated by the pilot phase as follows:

$$\hat{\theta}^{(p)}_{ML} = \arg\left\{\sum_{k=0}^{N_p} C^{(p)^*}(k) S^{(p)}(k)\right\}. \tag{9}$$

$$C^{(p)^*} = \frac{1}{T_s}\int_0^{T_s} r(t-iT_s)S^*(k)\mathrm{d}t$$

designates the conjugate of $C^{(p)}(k)$ which designates the pilot carrier symbols that are overhead (they do not carry any information content).

When a signal sample $S^{(p)}(k)$ corresponding to a pilot signal reaches the receiver, it is retrieved by the receiver and the above equation is computed sample by sample as illustrated in Fig. 4. Mathematically, this can be translated as the following equation

$$S(t) = c^1_{1i}s^1_{1i}(t-iT_s) + c^2_{2i}s^2_{2i}(t-iT_s) + c^3_{3i}s^3_{3i}(t-iT_s) + \ldots$$

$$+ c^k_{ki}s^k_{ki}\left(t-iT_s\right) + \cdots + c^N_{Ni}s^N_{Ni}(t-iT_s).$$

Then rewritten as

$$S(t) = \sum_{i=-\infty}^{+\infty}\sum_{k=1}^{N} C_{ki}S_k(t-iT_s), \tag{10}$$

$S(t)$ (which is denoted as $X(k)$ in Eq. (1)) is the OFDM multi-carrier modulation transmitted signal.

4 M-QAM constellations, simulation results

The pilot-data-aided feed forward carrier phase jitter recovery (PA FF CPJR) has been investigated for square

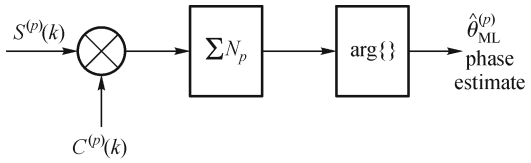

Fig. 4 Illustration of PA FFML for CPJR

m-ary QAM formats 4-QAM (or QPSK), 16-QAM, 64-QAM and 256-QAM. These square constellations are the easiest to generate [19] and are optimally immune against additive white Gaussian noise [20].

We compared three types of coherent OFDM receivers: a noise-free receiver (the ideal receiver), a receiver using PA FF CPJR without ML, and a receiver using PA FF CPJR with ML. Ideal receiver means a noise-free receiver in a simulation that knows the exact carrier phase achieved. In this kind of receiver, the penalty sensibility is caused only by quantization effects.

A computer simulation was used to verify the effectiveness of the PA FF carrier recovery employing ML in a CO-OFDM system at a 10 Gb/s transmission rate. OFDM system parameters used for the simulation are: number of subcarriers $N = 512$, FFT points = 1024, transmission link 1600 km standard single mode fiber (SSMF), sampling rate 1 GS/s and sampling period $T_s = 1$ ns, symbol period of 25.8 ns and guard time of 3.5 ns. All our simulation was based on each data point of 2000 OFDM symbols. The system is assumed to be free ISI.

4.1 M-QAM phase noise tolerance

PA FF with/without ML and a noise-free receiver (ideal receiver) are simulated to verify the performance of the new estimation method in terms of laser linewidth tolerance using square M-QAM schemes.

The sensibility penalty of optical signal to noise ratio (OSNR) as a function of phase error variance for 4-QAM, 16-QAM, 64-QAM and 256-QAM is shown respectively in Figs. 5(a)–5(d). It is shown that PA FFML performs much like a noise-free receiver and improves the linewidth tolerance when the phase error variance increases. Hence this demonstrates the effectiveness of the new estimation scheme for phase jitter recovery.

A quantitative performance of the new method in terms of linewidth tolerance is resumed in Table 1.

For higher QAM constellations, the efficiency of the phase estimation reduces. This can be related to the fact that for lower OSNR other limiting factors like quantization and phase noise become more dominant.

4.2 Bit error rate sensitivity

In Fig. 6, we compared BER sensitivity versus OSNR for different QAM constellations using the CPJR with FFML.

Relation between theoretical expressions of OSNR and BER is given by [15]

$$\frac{E_s}{N_0} = \frac{M-1}{3}\left(Q^{-1}\left(\frac{\log_2 M}{2}\left(1-\frac{1}{\sqrt{M}}\right)^{-1}\left(1-\sqrt{1-\mathrm{BER}}\right)\right)\right)^2, \tag{11}$$

where, E_s/N_0 is the OSNR, M is the number of constellation points, BER is the target bit error rate and $Q(x) = \frac{1}{2}\mathrm{erfc}\left(\frac{x}{\sqrt{2}}\right)$ is the Q function.

From Eq. (11), the BER is given by

$$\mathrm{BER} = 1-\left(1-\frac{2}{\log_2 M}\left(1-\frac{1}{\sqrt{M}}\right)Q\left(\sqrt{\frac{3}{M-1}\frac{E_s}{N_0}}\right)\right)^2. \tag{12}$$

Figure 6 shows that 4-QAM attains a maximum BER of 2×10^{-2}. For 16-QAM, a maximum BER of 3×10^{-2} is attained. The maximum penalty for 64-QAM is 6×10^{-2}, while 8×10^{-2} BER is attained for 256-QAM.

4.3 Impact of ADC resolutions on receiver performance

This part studies the effect of ADC resolutions on the system performance using PA FFML with different square M-QAM constellations. Figure 7 shows the Q-factor penalty versus different ADC resolutions.

From Fig. 7, it is noticed that there is a positive variation of Q factor ($\Delta Q = 1.5$) for 4-QAM, while 16-QAM, 64-QAM and 256-QAM attain respectively the following positive variations of Q factor: 2.5, 3.5 and 5.5. In other terms, 4-QAM is less sensible to big values of ADC resolutions compared to 16-QAM, 64-QAM and 256-QAM.

5 Conclusions

This paper demonstrated the use of PA FF CPJR in CO-OFDM employing square arbitrary M-QAM constellations as modulation formats. We introduced a new pilots arrangement in two congruent diagonals of OFDM frame leading to highly accurate, interpolation-free phase estimation. It is shown by mathematical deduction how the pilot's phase is extracted at the receiver and used for phase estimation. The performance of the new method was demonstrated through simulations. The introduction of ML in PA FF was shown to be beneficial for the system. The

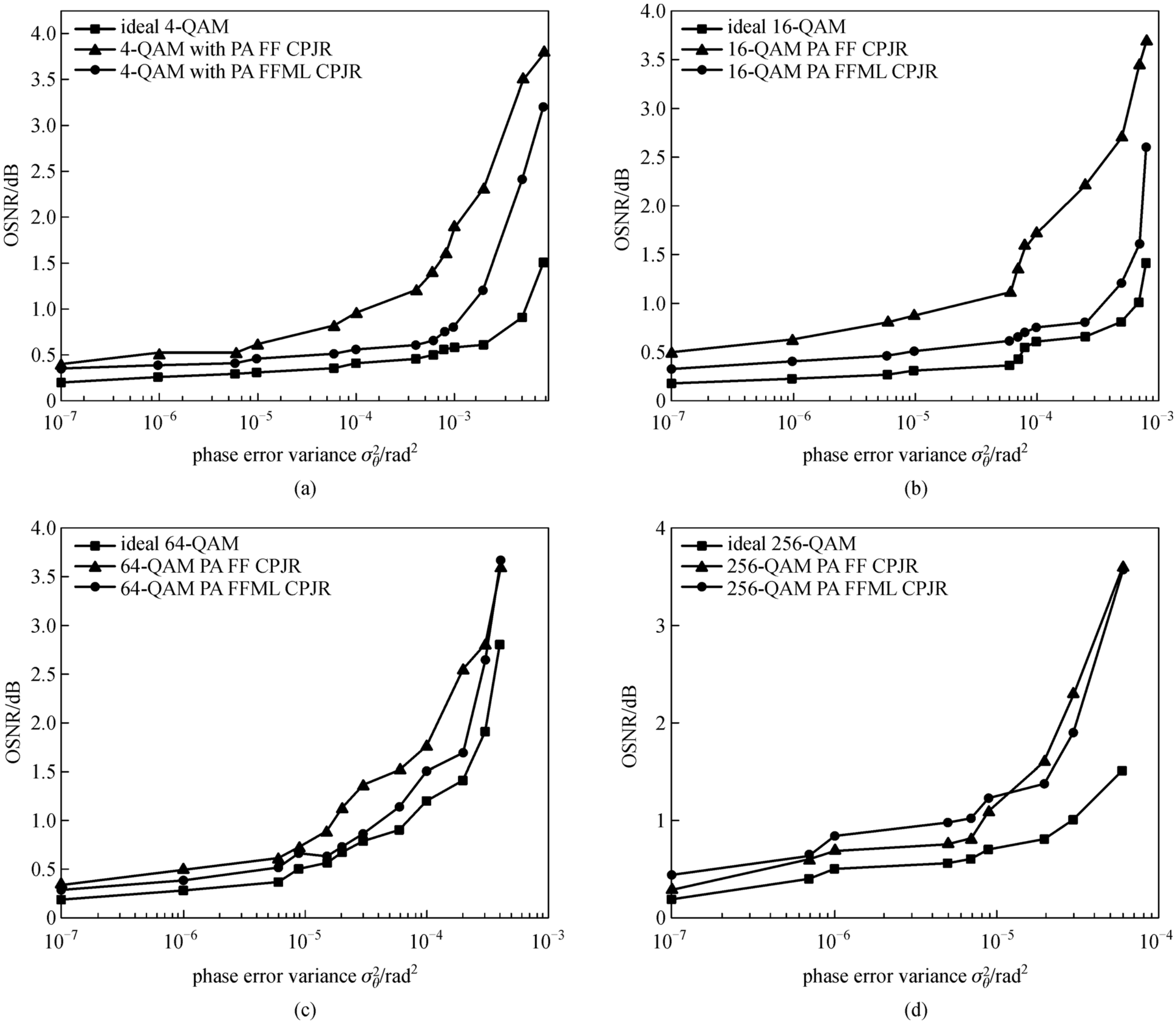

Fig. 5 Penalty sensitivity for CO-OFDM noise-free receiver, PA FF CPJR receiver and PA FFML CPJR receiver. (a) 4-QAM (QPSK); (b) 16-QAM; (c) 64-QAM; (d) 256-QAM

Table 1 Linewidth requirements for PA FF CPJR with different square QAM constellations for OSNR = 1 dB

phase recovery techniques	4-QAM (QPSK)		16-QAM		64-QAM		256-QAM	
	max tolerable σ_θ^2 for 1 dB at BER = 10^{-3}	max tolerable Δf for $\frac{1}{T_s} = 1$ Gbaud	max tolerable σ_θ^2 for 1 dB at BER = 10^{-3}	max tolerable Δf for $\frac{1}{T_s} = 1$ Gbaud	max tolerable σ_θ^2 for 1 dB at BER = 10^{-3}	max tolerable Δf for $\frac{1}{T_s} = 1$ Gbaud	max tolerable σ_θ^2 for 1 dB at BER = 10^{-3}	max tolerable Δf for $\frac{1}{T_s} = 1$ Gbaud
ideal receiver	56.55×10^{-3}	9 MHz	56.55×10^{-4}	0.9 MHz	53.40×10^{-5}	85 kHz	31.42×10^{-5}	50 kHz
PA FF CPJR	6.28×10^{-4}	0.1 MHz	3.14×10^{-5}	5 kHz	15.71×10^{-5}	25 kHz	50.27×10^{-6}	8 kHz
PA FFML CPJR	9.42×10^{-3}	1.5 MHz	6.28×10^{-4}	0.1 MHz	44×10^{-5}	70 kHz	44×10^{-6}	7 kHz

Note: BER stand for bit error rate

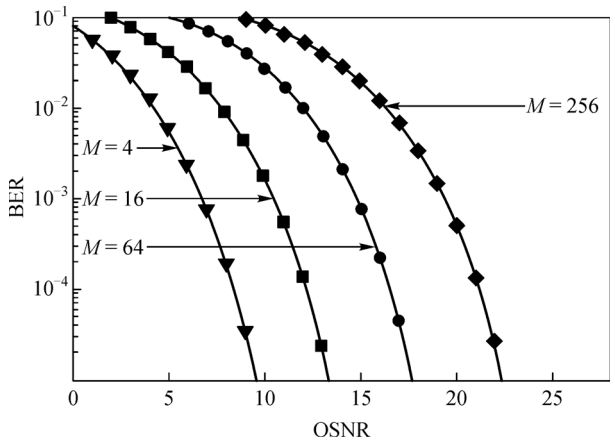

Fig. 6 BER performance comparison for different square M-QAM PA FF CPJR impacted by phase noise

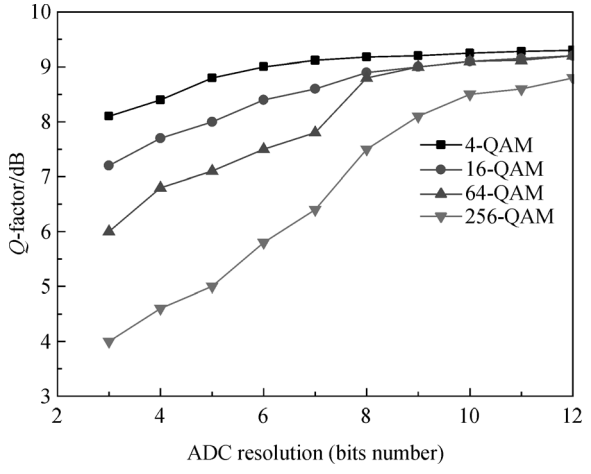

Fig. 7 Impact of ADC resolutions on receiver sensitivity of CO-OFDM using square-QAM and PA FFML CPJR

phase error variance leading to 1-dB penalty was found to be $9.42 \times 10^{-3}\text{rad}^2$ (4-QAM or QPSK), $6.28 \times 10^{-4}\text{rad}^2$ (16-QAM), $44 \times 10^{-5}\text{rad}^2$ (64-QAM) and $44 \times 10^{-6}\text{rad}^2$ (256-QAM). BER versus OSNR simulations indicated that 4-QAM performs better. The impact of resolutions on system performance was studied. It was found that 4-QAM is immune to ADC resolutions. In contrast, the other three square QAM constellations performed poorly with small ADC resolution values and the effect of infinite ADC resolutions values was negligible.

In conclusion, simulations have shown that LO laser linewidth is involved in the quality of signal reception and 4-QAM outperforms 16-QAM, 64-QAM and 256-QAM. Moreover, with the new phase jitter estimation method, it is straightforward to interpolate the phase jitter with minimum mean square error at the receiver and thus the synchronization of CO-OFDM receiver can be achieved. This synchronization can improve the performance of CO-OFDM.

References

1. Sun H, Wu K T, Roberts K. Real-time measurements of a 40 Gb/s coherent system. Optics Express, 2008, 16(2): 873–879
2. Roberts K, O'Sullivan M, Wu K T, Sun H, Awadalla A, Krause D J, Laperle C. Performance of dual-polarization QPSK for optical transport systems. Journal of Lightwave Technology, 2009, 27(16): 3546–3559
3. Shieh W, Djordjevic I. OFDM for optical communications. Access Online via Elsevier
4. Winzer P J. Beyong 100 G ethernet. IEEE Communications Magazine, 2010, 48(7): 26–30
5. Agrawal G P. Fiber-Optic Communication Systems. 3rd ed, Hoboken: John Wiley & Sons, Inc., 2002
6. Zhang X, Pang X, Deng L, Zibar D, Monroy I T, Younce R. High phase noise tolerant pilot-tone-aided DP-QPSK optical communication systems. Optics Express, 2012, 20(18): 19990–19995
7. Temga J, Zhang M M, Liu D M. Influence of sampling jitter effects on the performance of OFDM in optical network. In: Proceedings of 3rd International Conference on Internet Technology and Application, 2012
8. Sliskovic M. Sampling frequency offset estimation and correction in OFDM systems. In: Proceedings of 8th IEEE International Conference on Electronics, Circuits and Systems, 2001, 437–440
9. Sliskovic M. Carrier and sampling frequency offset estimation and correction in multicarrier systems. In: Proceedings of IEEE Global Telecommunications Conference, 2001, 285–289
10. Jansen S L, Morita I, Schenk T C W, Takeda N, Tanaka H. Coherent optical 25.8-Gb/s OFDM transmission over 4160-km SSMF. Journal of Lightwave Technology, 2008, 26(1): 6–15
11. Giddings R, Tang J. World-first experimental demonstration of synchronous clock recovery in an 11.25 Gb/s real-time end-to-end optical OFDM system using directly modulated DFBs. In: Proceedings of Optical Fiber Communication Conference, 2011
12. Giddings R P, Tang J M. Experimental demonstration and optimisation of a synchronous clock recovery technique for real-time end-to-end optical OFDM transmission at 11.25 Gb/s over 25 km SSMF. Optics Express, 2011, 19(3): 2831–2845
13. Shieh W, Yi X, Tang Y. Transmission experiment of multi-gigabit coherent optical OFDM systems over 1000 km SSMF fibre. Electronics Letters, 2007, 43(3): 183–185
14. Pfau T, Peveling R, Hauden J, Grossard N, Porte H, Achiam Y, Hoffmann S, Ibrahim S, Adamczyk O, Bhandare S, Sandel D, Porrmann M, Noé R. Coherent digital polarization diversity receiver for real-time polarization- multiplexed QPSK transmission at 2.8 Gbit/s. IEEE Photonics Technology Letters, 2007, 19(24): 1988–1990
15. Tang Y, Shieh W, Yi X, Evans R. Optimum design for RF-to-optical up-converter in coherent optical OFDM Systems. IEEE Photonics Technology Letters, 2007, 19(7): 483–485
16. Temga J, Zhang M M, Liu D M, He W L. Performance analysis of coherent optical OFDM with weiner phase noise jitters. In: Proceedings of Information Optoelectronics, Nanofabrication and Testing, 2012
17. Ip E, Lau A P T, Barros D J F, Kahn J M. Coherent detection in

optical fiber systems. Optics Express, 2008, 16(2): 753–791
18. Oppenheim A V, Shalfer R W, Buck J R. Discrete-Time Signal Processing. 2nd ed. New Jersey: Prentice-Hall, 1999
19. Lu G W, Sköld M, Johannisson P, Zhao J, Sjödin M, Sunnerud H, Westlund M, Ellis A, Andrekson P A. 40-Gbaud 16-QAM transmitter using tandem IQ modulators with binary driving electronic signals. Optics Express, 2010, 18(22): 23062–23069
20. Pfau T, Hoffmann S, Noe R. Hardware-efficient coherent digital receiver concept with feedforward carrier recovery for M-QAM constellations. Journal of Lightwave Technology, 2009, 27(8): 989–999

Jean Temga received the Bachelor of Science (with honors) in Physics from the University of Ngaoundere, Adamawa, Cameroon, in 2006 and the Master of Engineering in Communication and Information Systems from Huazhong University of Science and Technology, Wuwhan, China, in 2009, where he is currently working toward the Ph.D degree in Optoelectronic Information Engineering in the School of Optics and Electronic Information. His research interests include optical orthogonal frequency division multiplexing (OFDM), optical communication systems, and optical signal processing in coherent receivers.

Deming Liu received the M.S. degree from University of Electronic Science and Technology of China and Ph.D degree from Huazhong University of Science and Technology in 1984 and 1999, respectively. He conducted research into the broadband access network at Nanyang Technological University in Singapore as a visiting researcher from 1999 to 2000. He is now a professor and serving as a Director of the National Engineering Laboratory for Next Generation Internet Access System.

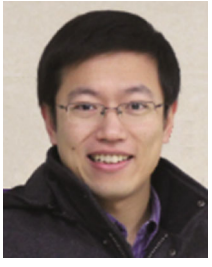

Minming Zhang received the B.S., M.S. and Ph. D degrees from Huazhong University of Science and Technology (HUST), Wuhan, China, in 1998, 2001 and 2009, respectively. In 2001, he became a faculty member with the School of Optics and Electronic Information of HUST, where he is currently an associate professor. His current research interests include photonic integrated technology for multi-wavelength laser emission, broadband wireless-over-fiber access systems and nonlinear photonic integrated devices.